# The Effect of Conformation on Membrane Permeability of an Acyloxyalkoxy-linked Cyclic Prodrug of a Model Hexapeptide

**Sanjeev Gangwar,[1] Seetharama D. S. Jois,[1] Teruna J. Siahaan,[1] David G. Vander Velde,[1] Valentino J. Stella,[1] and Ronald T. Borchardt[1,2]**

*Received June 14, 1996; accepted August 23, 1996*

***Purpose.*** To determine the different conformations of the acyloxyalkoxy-linked cyclic prodrug 1 of the model hexapeptide 2 in solution and to investigate the relationship between these solution conformations and the cellular permeability characteristics of this prodrug.

***Methods.*** Two-dimensional Homonuclear Hartmann-Hahn spectroscopy, Rotating-Frame Overhouser effect spectroscopy, circular dichroism and molecular dynamics simulations were used to find the solution conformers of cyclic prodrug 1.

***Results.*** Our spectroscopic findings suggest that cyclic prodrug 1 exhibits a major and a minor conformer in solution. The major conformer appears to have a well-defined secondary structure, which involves a β-turn and 4 → 1 intramolecular hydrogen bond, creating a compact structure with a reduced average hydrodynamic radius compared to the model hexapeptide 2.

***Conclusions.*** The increased ability of cyclic prodrug 1 to permeate membranes compared to the model hexapeptide 2 could be due to reduction in the average hydrodynamic radius of the molecule facilitating paracellular flux and/or the reduction in the hydrogen bonding potential facilitating transcellular flux.

**KEY WORDS:** esterase-sensitive prodrug; peptide delivery; membrane permeability; solution conformation; nuclear magnetic resonance spectroscopy; circular dichroism.

## INTRODUCTION

In general, peptide drugs have very poor permeation through biological membranes, which limits their potential use as therapeutic agents. The physicochemical characteristics of a molecule that favor permeability include decreased molecular size (1), reduced charge (2), increased lipophilicity (3, 4) and reduced hydrogen bonding potential (5, 6). Therefore, a solution conformation that allows the optimization of one or more of these characteristics may facilitate permeation across biological membranes.

In an earlier study, using an *in vitro* cell culture model of the intestinal mucosa, our laboratory (7) showed that cyclic prodrug 1 was substantially more able to permeate than the corresponding linear hexapeptide 2 (Figure 1). This increased permeation was due, in part, to the increased metabolic stability of 1 compared to 2. However, even when the hexapeptide 2 was stabilized to metabolism using protease inhibitors (7) or by chemical modification (8), its permeation was still substantially less than that of cyclic prodrug 1. Characterization of the physicochemical properties of these peptides showed that cyclic prodrug 1 had a smaller molecular radius and an increased lipophilicity compared to the hexapeptide 2 (7).

In this study, we have determined the solution conformations of cyclic prodrug 1 in an attempt to explain this reduced molecular radius and increased lipophilicity. In addition, we have attempted to explain the relationship between the solution conformation of the molecule, its physicochemical properties and its cell monolayer permeability characteristics.

## MATERIAL AND METHODS

### Synthesis

Cyclic prodrug 1 (Fig. 1) was synthesized by the solution phase method using standard Boc-amino acid chemistry. The details of the syntheses have been published elsewhere (9).

### NMR Spectroscopy

Samples of the cyclic prodrug 1 for NMR experiments were prepared by dissolving 5 mg of peptide in 500 μL of 90% $H_2O$ and 10% $D_2O$ at pH 3.5. The one- and two-dimensional NMR experiments were carried out using 500 MHz Brüker AM-500 and Varian XL300 MHz NMR spectrometers equipped with variable temperature probes. Homonuclear Hartmann-Hahn (HOHAHA) experiments were done by presaturation of

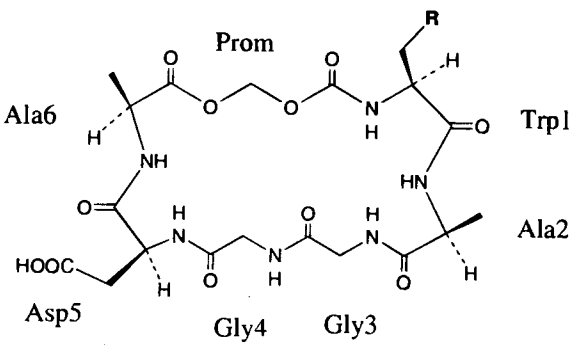


H-Trp-Ala-Gly-Gly-Asp-Ala-OH

2

**Fig. 1.** Chemical structures of the acyloxyalkoxy-linked cyclic prodrug 1 and model hexapeptide 2.

[1] Department of Pharmaceutical Chemistry, 2095 Constant Ave., The University of Kansas, Lawrence, Kansas 66047.

[2] To whom correspondence should be addressed.

**ABBREVIATIONS:** NMR, nuclear magnetic resonance; CD, circular dichroism; CCA method, convex constraint analysis method; HOHAHA, Homonuclear Hartmann-Hahn spectroscopy; ROESY, rotating frame nuclear Overhauser effect spectroscopy; NOESY, nuclear Overhauser enhancement and exchange spectroscopy; NOE, nuclear Overhauser enhancement; TPPI, time proportional phase incrementation; DQF-COSY, double quantum filtered correlated spectroscopy; Cvff, consistence valence force field; MD, molecular dynamics.

water during relaxation delay. Data were collected in time proportional phase incrementation (TPPI) with a sweep width of 5000 Hz. Typically, 48 or 64 scans were collected with 2K data points in the $t_2$ dimension and 256 or 300 experiments in the $t_1$ dimension. Nuclear Overhauser enhancement and exchange spectroscopy (NOESY) experiments were recorded with mixing times in the range of 150 to 500 ms. Nuclear Overhauser enhancement (NOE) cross-peaks were of weak intensity. Therefore, rotating frame nuclear Overhauser effect spectroscopy (ROESY) experiments (10) were carried out with 250 and 400 ms spin lock times at 10°C. Data sets consisting of 512 $t_1$ increments of 2K complex data points were collected for double quantum filtered correlated spectroscopy (DQF-COSY) experiments. NMR spectra were processed using FELIX software (version 2.30, Biosym Technologies, San Diego, CA) with a final matrix of 1K × 1K real data points. A sine bell filter shifted by either 45° or 60° was used in both dimensions prior to Fourier transformation. Baseline corrections were applied after phase correction using the convolution method available in the FELIX software. Spectra were represented in the absorption mode in the case of NOESY and the phase-sensitive mode in the case of DQF-COSY experiments.

The temperature-dependence of the amide proton chemical shift was measured by collecting data from 10 to 40°C in steps of 5°C using a variable temperature probe. Coupling constants ($^3J_{HN\alpha}$) were measured from the DQF-COSY spectrum at 10°C. ROE cross-peak volumes were measured using the ROESY spectrum with 250 ms mixing time; intensities were assigned as strong, medium and weak. The upper bounds of distances for $d_{N\alpha}$ $(i, i)$, $d_{\alpha N}$ $(i, i + 1)$ and $d_{NN}$ $(i, i + 1)$ were assigned values of 3.0 Å, 3.6 Å and 4.5 Å, respectively. Side chain protons were not stereospecifically assigned; hence, ROE restraints for side chain protons were calculated by considering pseudo atoms (11).

## Computational Methods

Conformational space was searched for this cyclic peptide using the Discover program (version 2.35, Biosym Technologies, San Diego, CA) to identify conformations consistent with the experimental ROE and coupling-constant data. Calculations were performed on an Indigo, Silicon Graphics computer. Consistence valence force field (Cvff) was used for these calculations. Initially, the peptide was cyclized using ROE constraints by running MD simulations *in vacuo* for 20 ps at 900 K with a dielectric constant of unity. A penalty force of 100 kcal $mol^{-1}$ $Å^{-2}$ was used to bring the protons to observable ROE distances. From the 20 ps MD simulations, peptides with reasonable peptide bond geometry were chosen. These structures were then subjected to 900 K MD for 100 ps to explore the possibility of several conformations that the peptide could acquire, and the trajectories were updated every 100 fs. During this high temperature simulation, all the peptide bonds were held *trans*, since the peptide does not contain proline residues or N-methylated residues (12). The trajectories from high temperature dynamics were analyzed for similarities between the structures by comparing the root mean square (r.m.s.) deviation between each possible pair of structures. The r.m.s. deviations between the backbone atoms were plotted in a 100 × 100 matrix with $x$ and $y$ axes representing structure numbers. Elements near the diagonal represented structures with low r.m.s. values. The plot showed (figure not shown) that there were a number of areas of clusters along the diagonal, indicating that several distinct structures were encountered during the MD simulations. These areas were divided into six conformational families. The r.m.s. deviation of the backbone atoms within the family compared to the average structure was 0.4 Å. Average structures from each family were taken and subjected to 100 steps of energy minimization, using the steepest descents method to relax the molecule. Each structure was then soaked with water molecules (sphere of radius of 15 Å) with the peptide molecule at the center of the sphere, followed by 100 ps MD simulations at 300 K with all the ROE constraints. Trajectories were updated every 100 fs during the MD simulations. Several conformations were selected for the final analysis using two criteria: a) that the conformation had an interproton distance error of less than 0.5 Å compared to upper and lower bounds of distances from ROE data; and b) that the conformation had angles within 30 degrees of the calculated values from $^3J_{HN\alpha}$. These were taken as viable NMR solution conformations and were minimized with solvent molecules using the conjugate gradient method without cross terms until the r.m.s. derivative was 0.4 kcal/mole-Å. The energy-minimized structures were analyzed in terms of dihedral angles, energy and observed ROE distances. Conformers were finally clustered into two families based on these structural characteristics ($\Phi$ and $\psi$ angles) and ROE constraints. An average structure that was consistent with the NMR data was chosen from each family.

## Circular Dichroism (CD)

CD experiments were performed using an AVIV CD-60DS. Samples for CD experiments of the prodrug 1 were prepared in methanol at a concentration of 0.5 mg/mL. Data were collected in the range of 280 to 190 nm in steps of 1 nm and smoothed. For secondary structure analysis, ellipticity values were taken every nanometer. CD data were evaluated by the convex constraint analysis method (CCA) to determine the percentage of secondary structure (13). Spectra were appended to the reference data set in the CCA program. Deconvolution of the spectra was carried out by assuming 3, 4 and 5 components to find the weight of different secondary structural elements of the peptide. The four component deconvolution resulted in the best fit with the experimental CD spectrum, and conformational weights were obtained from this analysis. The component curves were assigned to different secondary structural elements such as α-helix, β-sheet or β-turn by comparison with the curves in the literature (14).

## RESULTS

The proton chemical shifts of cyclic prodrug 1 (Table I) were identified from the 2D-HOHAHA (Fig. 2.A) spectrum. Sequence-specific assignments were made from the ROESY spectrum (Fig. 2.B) using standard procedures (11). The one-dimensional $^1H$ NMR spectrum of the cyclic prodrug 1 showed good dispersion of the chemical shifts and the coupling patterns, indicative of a stable major conformer at the experimental temperature. Most of the amide resonances had coupling constants greater than 5 Hz. The one-dimensional spectrum also showed additional peaks that could be due to a minor conformer. The intensity of minor resonances did not increase with changes in either temperature or solvent system (DMSO). These minor resonances might arise due to flexibility around the promoiety.

**Table I.** Temperature Coefficient, Coupling Constant, and Chemical Shift Data for the Cyclic Prodrug 1 in 90% $H_2O$ and 10% $D_2O$ at 10°C

| Residue | $\Delta\delta/\Delta T$ (ppb/K) | Coupling Constant $^3J_{HN\alpha}$(Hz) | Chemical Shift (in ppm) NH | $C^\alpha H$ | $C^\beta H$ |
|---|---|---|---|---|---|
| Trp1 | 8.2 | 5.8 | 7.45 | 4.42 | 3.33 |
| Ala2 | 6.4 | 6.4 | 8.19 | 4.12 | 1.03 |
| Gly3 | 3.0 | 12.7[a] | 7.81 | 3.77/4.16 | |
| Gly4 | 9.4 | 11.4[a] | 8.49 | 3.81/3.96 | |
| Asp5 | 9.4 | 6.7 | 8.46 | 4.57 | 2.71 |
| Ala6 | 7.2 | 7.2 | 8.07 | 4.38 | 1.43 |

[a] In the case of Gly, it is $^3J_{HNC^\alpha H2}$ (Hz).

Ambiguities in the assignment of resonances of amino acids occurring twice in the sequence were resolved using HOHAHA as well as ROESY spectrum cross-peak connectivities. A ROESY spectrum was also used to distinguish NOE and exchange peaks. Some of these exchange peaks are very strong, indicating a fast exchange rate. It is often observed that conformations with small populations are easily observed by strong exchange cross peaks (15). The Gly3 and Gly4 proton resonances can be distinguished from each other using their NH to $C^\alpha H$ and NH-NH sequential connectivities in the ROESY spectrum. The NH of Gly3 showed through-space interaction with the NH of Ala2, while the NH of Asp5 showed through-space interaction with the NH of Ala6. The proton resonances of Ala2 and Ala6 were distinguished by their NH-NH connectivity to Gly3 and Asp5, respectively. HOHAHA and ROESY spectrum also showed additional cross-peaks, labeled as "*m*," which could be due to the minor conformer.

Twenty-six intra- and inter-residue ROEs were observed in the cyclic prodrug 1. The ROESY spectrum also showed some additional cross peaks, labeled as "*e*," that were due to

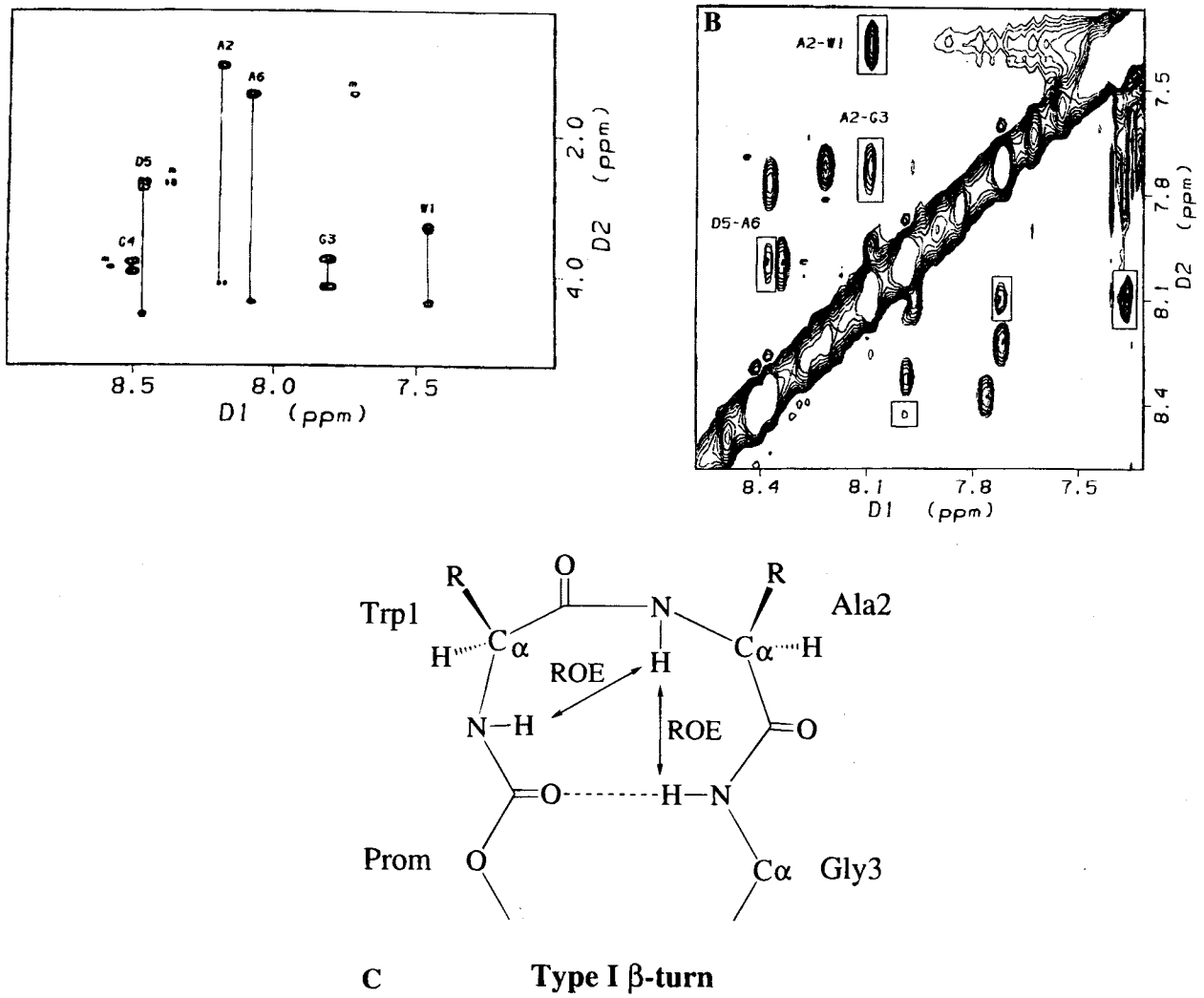


**Fig. 2.** Structural analysis of the cyclic prodrug 1 by NMR spectroscopy. Panel A shows the 500 MHz $^1H$ NMR HOHAHA spectrum of cyclic prodrug 1 in 90% $H_2O$ and 10% $D_2O$ at 70 ms mixing time at 10°C. Cross-peaks between amide protons and $H^\alpha$and $H^\beta$ protons are shown with assignments (*m* indicates cross peaks due to minor conformer). Panel B shows the expansion of the amide region of ROESY spectrum of the cyclic prodrug 1 at 250 ms mixing time at 10°C showing sequential connectivities. Cross-peaks are opposite in phase to diagonal peaks (*e* indicates the exchange peaks between conformers). Panel C shows the schematic representation of ROEs and hydrogen bonding.

**Table II.** Backbone Dihedral Angles (in deg) for the Conformation of Cyclic Prodrug 1. Possible Dihedral Angles Calculated from the Coupling Constants Are also Tabulated for Comparison

| Residue | Calculated Φ | Average Structure Φ | Ψ |
|---|---|---|---|
| Trp1 | −170, −75, 20, 95 | −72 | −37 |
| Ala2 | −168, −75, 25, 95 | −56 | −20 |
| Gly3 | −124, −60, 60, 120 | −75 | −64 |
| Gly4 | −130, −56, 56, 130 | −169 | −77 |
| Asp5 | −165, −75, 30, 45 | −105 | −70 |
| Ala6 | −160, −80, 35, 85 | −92 | 129 |

the exchange of amide protons between the major and minor conformers (Fig. 2.B). The NH of Trp1 showed connectivity to the NH of Ala2, and the NH of Ala2 displayed connectivity to the NH of Gly3. This result suggests a possible β-turn at Prom-Trp1-Ala2-Gly3. One of the possible dihedral (Φ) angles of Ala2 from $^3J_{HN\alpha}$ is −75 degrees (Table II), which is consistent with its $i + 2$ position in I β-turn. The temperature coefficients of the amide proton chemical shifts are shown in Table I. Most of the amide protons have a very large temperature coefficient of chemical shift, indicative of the presence of solvent-exposed amide protons. The NH of Gly3 showed a suppressed temperature coefficient, suggesting an intramolecularly hydrogen-bonded amide. The Gly3 $C^{\alpha}H$ enantiotopic proton resonances have a Δδ of about 0.4 ppm, indicating that these protons are in a different chemical environment, whereas the Gly4 protons have a Δδ of about 0.1 ppm, indicating the average environment. These data also support the fact that Gly4 is in a flexible part of the molecule, while Gly3 is in a region of well-defined secondary structure.

The calculated and experimental circular dichroism spectra of the cyclic prodrug 1 are shown in Figure 3. The CD spectrum was processed and deconvoluted to give four components, and conformational weights were obtained for each of the components. The component curves were assigned to different secondary structural elements such as α-helix, β-sheet or β-turn by comparison with the curves in the literature (14). The conformational weights for the β-turn and unordered structures were approximately 60% and 35%, respectively. In the case of the β-turn, the deconvoluted curve was assigned to a type I β-turn by comparison with the curves in the literature (14).

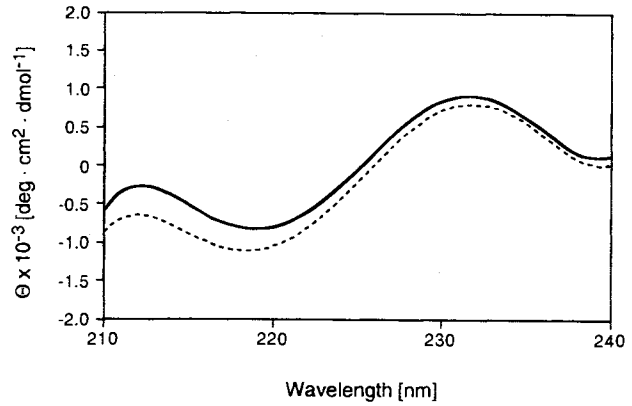


**Fig. 3.** CD spectrum of cyclic prodrug 1 in methanol (solid lines indicate experimental spectra and dotted lines indicate calculated spectrum; $\sigma = 0.078$).

The spectroscopic data strongly indicated the existence of a β-turn structure. From the ROE-constrained molecular dynamics simulation and energy minimization study, a family of structures was selected. These structures were consistent with the NMR data. A total of twelve conformers were then selected from this family and were superimposed onto the average structure to verify convergence with the average structure. The average r.m.s. deviation of the backbone and of all atoms was not more than 0.7 Å and 1.2 Å, respectively. The energy-minimized average structure, as shown in Figure 4, represents the possible major solution conformer of prodrug 1. The dihedral angles Φ of all the residues are within 40 degrees of those Φ angles calculated from the coupling constant data in the average structure (Table II) (16).

## DISCUSSION

Cyclic prodrug 1 was found to be substantially more able to permeate a cell monolayer ($P_{app} = 12.97 \pm 1.48 \times 10^{-8}$ cm/sec) than the linear hexapeptide 2 ($P_{app} < 0.17 \times 10^{-8}$ cm/sec) (7). The low permeation of hexapeptide 2 was due in part to its high susceptibility to enzymatic degradation by peptidases present in the Caco-2 cell monolayer ($t_{1/2} = 14$ min) (7). However, even when the linear hexapeptide 2 was stabilized to rapid metabolism using a cocktail of potent peptidase inhibitors, it was still substantially less able to permeate ($P_{app} = 4.05 \pm 0.24 \times 10^{-8}$ cm/sec) than was cyclic prodrug 1 (7). The metabolic stability of the linear hexapeptide 2, in the presence of peptidase inhibitors, and the permeation ($P_{app} = 3.16 \pm 0.27 \times 10^{-8}$ cm/sec) of a chemically modified N- and C-terminal capped linear hexapeptide were found to be similar (8).

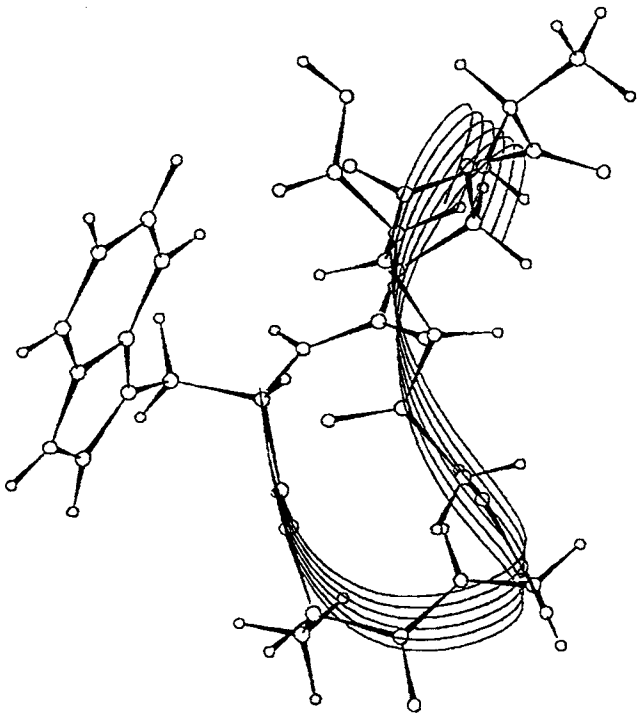

**Fig. 4.** ROE constrained and energy-minimized, average representative structure for cyclic prodrug 1.

Our hypothesis for the increased permeation of cyclic prodrug 1 was that the prodrug adopts conformations that favor the formation of intramolecular hydrogen bonds, making the molecule more lipophilic. This increases its transcellular flux and/or makes it more compact, thus increasing its paracellular flux. In an earlier study, our laboratory has demonstrated that the linear hexapeptide 2 and the N- and C-terminal capped linear hexapeptide exist in dynamic equilibrium between random coil (major) and various turn structures (8). Therefore, this study was undertaken to determine solution structures of the cyclic prodrug 1 in water.

The spectroscopic data of cyclic prodrug 1 strongly suggest the existence of a β-turn structure. The average structure of the prodrug is stabilized by an intramolecular hydrogen bond between the NH of Gly 3 and C=O of the promoiety. The dihedral angles at Trp1 and Ala2 indicated that there is a type I β-turn at Prom-Trp1-Ala2-Gly3 (17). The presence of intramolecular hydrogen bonding is also supported by a low temperature coefficient of chemical shift of Gly3 NH. The β-turn is also supported by the presence of ROE between the NH of Trp1 and Ala2 and the NH of Ala2 to Gly3. The average structure also showed hydrogen bonding between the Gly4 NH (5 → 1) and the C=O of the promoiety. This (5 → 1) hydrogen bonding causes a twist around the Gly4 residue and flips over the rest of the molecule, making it even more compact. However, this hydrogen bonding was not observed in the temperature coefficient data for the Gly4 residue. Therefore, the average structure of the cyclic prodrug 1 appears to be compact (3.6 Å average molecular radius), has a well-defined β-turn structure at Prom-Trp1-Ala2-Gly3, and has intramolecular hydrogen bonds.

The majority of drugs cross the intestinal epithelium to their site of action via the transcellular route. However, peptides show very limited passive transcellular diffusion because of the large number of functional groups present in the peptide backbone that hydrogen bond to water. The rate-limiting step for the transcellular pathway is desolvation of the solute, which allows the molecule to enter the hydrophobic interior of the membrane. Burton and co-workers (5, 6) have shown that reduction in the hydrogen bonding potential of amide bonds improves the transport of peptides across Caco-2 cell monolayers. The average structure of prodrug 1 in aqueous solution showed an intramolecular hydrogen bonding between the Gly3 NH (4 → 1) and the C=O of the promoiety that was not present in the linear hexapeptide 2. Formation of this intramolecular hydrogen bond in prodrug 1 may account for an overall increased lipophilicity, as determined by IAM chromatography (7), thus increasing the transcellular flux via the passive diffusion route.

Some peptide drugs are assumed to permeate the intestinal mucosa via the paracellular pathway, an aqueous extracellular route across the epithelia (18). Structural features such as molecular size and charge play a significant role due to the size restrictions of the junctional complex. The pore radius in the Caco-2 cells which is accessible for the paracellular route, has been estimated to be between 5 and 6 Å (19). Consequently, peptides that follow the paracellular route must be smaller than 6 Å (molecular radius) to diffuse through. The average hydrodynamic radius of cyclic prodrug 1 was found to be smaller than that of the linear hexapeptide, as observed by size-exclusion chromatography (7). This reduction in average hydrodynamic radius could be due to the compactness that arises as a result of the well-defined secondary structure of prodrug 1 in solution. The increased ability of the cyclic prodrug 1 to permeate membranes compared to the linear hexapeptide 2 could be due to smaller average hydrodynamic radius, thus increasing the paracellular flux via the aqueous pores.

In summary, CD and NMR spectroscopy techniques were used to characterize the solution structure of prodrug 1. On the basis of these data and molecular dynamics simulations, we have shown that cyclic prodrug 1 exhibits a well-defined secondary structure involving a β-turn and 4 → 1 hydrogen bonding in water. These conformational features might be responsible for the increased lipophilicity and smaller average size of prodrug 1. The increased ability of cyclic prodrug 1 to permeate membranes compared to the linear hexapeptide (WAGGDA) could be due to a reduction in the average hydrodynamic radius of the molecule, thus increasing paracellular flux, and/or to a reduction in hydrogen bonding potential, leading to an increase in passive diffusion via the transcellular route.

In conclusion, we have described a novel strategy for preparing cyclic prodrugs of peptides that have increased metabolic stability and increased cell membrane permeability when compared to the linear peptides. However, it should be feasible to use this strategy to cyclize other biologically active peptides by linking the C-terminal carboxyl group to a side-chain amino (*e.g.*, Lys, Arg) or hydroxyl (*e.g.*, Ser, Thr, Tyr) group, or by linking a side-chain carboxyl group (*e.g.*, Asp, Glu) to a side chain amino (*e.g.*, Lys, Arg) or hydroxyl (*e.g.*, Ser, Thr, Tyr) group or other peptide mimetics. The application of this methodology to biologically active peptides (*e.g.*, opioid peptides) is currently under investigation in our laboratory.

## ACKNOWLEDGMENTS

Financial support was provided by the United States Public Health Service (DA09315) and Glaxo Inc. The authors would like to thank Dr. G. D. Fasman of Brandeis University for kindly providing us with the CCA software for CD data analysis.

## REFERENCES

1. S. S. Davis. In S. S. Davis, L. Illum, and E. Tomlinson (eds.), *Delivery Systems for Peptide Drugs*, Plenum Press, New York, 1986, pp. 1–21.
2. M. J. Humphrey. In S. S. Davis, L. Illum, and E. Tomlinson (eds.), *Delivery Systems for Peptide Drugs*, Plenum Press, New York, 1986, pp. 139–151.
3. W. T. Cefalu and W. M. Pardridge. *J. Neurochem.* **45**:1954–1956 (1985).
4. H. D. Kleinert, S. H. Rosenberg, W. R. Baker, H. H. Stein, V. Klinghofer, J. Barlow, K. Spina, J. Polakowski, P. Kovar, J. Cohen, and J. Denissen. *Science* **257**:1940–1943 (1992).
5. R. A. Conradi, A. R. Hilgers, N. F. H. Ho, and P. S. Burton. *Pharm. Res.* **9**:435–439 (1992).
6. P. S. Burton, R. A. Conradi, A. R. Hilgers, N. F. H. Ho, and L. L. Maggiora. *J. Control. Release* **19**:87–98 (1992).
7. G. M. Pauletti, S. Gangwar, F. W. Okumu, T. J. Siahaan, V. J. Stella, and R. T. Borchardt. *Pharm. Res.* **13**:1613–1621 (1996).
8. F. W. Okumu, G. M. Pauletti, D. G. Vander Velde, T. J. Siahaan, and R. T. Borchardt. *Pharm. Res.* **12**:S-302 (1995).
9. S. Gangwar, G. M. Pauletti, T. J. Siahaan, V. J. Stella, and R. T. Borchardt. *J. Org. Chem.* (submitted).
10. A. Bax and D. G. Davis. *J. Magn. Reson.* **63**:207–213 (1985).
11. K. Wüthrich. *NMR of Proteins and Nucleic Acids*, Wiley, New York, 1986.
12. G. N. Ramachandran and A. K. Mitra. *J. Mol. Biol.* **107**:85–92 (1976).

13. A. Perczel, K. Park, and G. D. Fasman. *Anal. Biochem.* **203**:83–93 (1992).
14. A. Perczel and G. D. Fasman. *Protein Science* **1**:378–395 (1992).
15. M. Kock, H. Kessler, D. Seebach, and A. Thaler. *J. Am. Chem. Soc.* **114**:2676–2686 (1996).
16. V. F. Bystrov. *Prog. NMR Spectros.* **10**;41–81 (1976).
17. G. D. Rose, L. M. Gierasch, and J. A. Smith. *Adv. Protein Chem.* **37**:1–109 (1985).
18. G. M. Pauletti, S. Gangwar, G. T. Knipp, M. M. Nerurkar, F. W. Okumu, K. Tamura, T. J. Siahaan, and R. T. Borchardt. *J. Control. Release* **41**:3–17 (1996).
19. G. T. Knipp, N. F. H. Ho, C. L. Barsuhn, and R. T. Borchardt. *Pharm. Res.* **12**:S-302 (1995).